

RESEARCH ARTICLE

Vulcanization of polypropylene

Callum Houghton-Flory | Mohand O. Saed | Eugene M. Terentjev Cavendish Laboratory, University of
Cambridge, Cambridge, UK**Correspondence**Eugene M. Terentjev, Cavendish
Laboratory, University of Cambridge,
JJ Thomson Avenue, Cambridge
CB3 0HE, UK.
Email: emt1000@cam.ac.uk**Funding information**HORIZON EUROPE European Research
Council, Grant/Award Number: 786659;
Royal Society, Grant/Award Number:
G113670**Abstract**

Dynamic covalent crosslinking of commodity thermoplastics is a desirable target in material development, as it promises to combine the enhanced mechanical properties and thermal/solvent stability of thermosets with reprocessability and plastic flow under certain conditions activating the bond exchange. Many attempts of this development suffer from the same two problems: enhanced cost due to complex and often toxic chemicals, and the effective melt-flow index being too low for practical use. Here we return to the origins of polymer networks, and mimic the vulcanization of natural rubber in the commodity polypropylene using elemental sulfur initiated by peroxide. Forming sulfur bridges allows easy catalyst-free reprocessability based on the disulfide bond exchange. We study a broad range of compositions and reaction conditions, finding optimal balance between the crosslinking and chain scission in the melt compounder, and demonstrating much enhanced characteristics of the resulting materials. We specifically discuss and evaluate the balance between the rubber-elastic network response at high temperatures and the plastic flow enabled by disulfide exchange, responsible for the reprocessing of our vitrimers.

KEYWORDS

disulfide bond exchange, plastic welding, sulfide bridging, vitrimers, vulcanization

1 | INTRODUCTION

Thermoplastic polyolefins (TPO) are ubiquitous in modern society with the most common being polyethylene (PE) and polypropylene (PP). Their daily use ranges from automotive and biomedical to household applications.¹ The production of TPO is rapidly growing and accounts for more than a half of the global plastic industry. Crosslinked thermoplastics, such as crosslinked polypropylene (XPP), are a class of materials that combine characteristics of both thermoplastics and thermosetting polymers. They exhibit unique properties that make them suitable for more demanding applications, particularly in situations where traditional thermoplastics might not offer the required

performance or stability levels. Crosslinking involves creating covalent bonds between polymer chains to enhance the material's mechanical, thermal, and chemical properties. Crosslinking prevents the material from melting or flowing when heated, unlike regular thermoplastics, while maintaining or enhancing the mechanical properties of the rigid plastic at ambient temperatures.

In the case of XPP, the plastic exhibits better heat resistance compared to standard PP, enhancing the range of applications. The crosslinking process improves the material's mechanical strength, toughness, and dimensional stability, as well as significantly reduced creep and stress relaxation. Crosslinking also increases resistance to chemicals and solvents, making XPP valuable in industries

This is an open access article under the terms of the [Creative Commons Attribution](https://creativecommons.org/licenses/by/4.0/) License, which permits use, distribution and reproduction in any medium, provided the original work is properly cited.

© 2024 The Authors. *Journal of Polymer Science* published by Wiley Periodicals LLC.

where exposure to harsh chemicals is common. In more specific settings, the improved thermal and electrical properties of XPP make it useful for electrical insulation purposes, such as cable insulation and connectors, as well as in applications where resistance to radiation, such as gamma or X-rays, is crucial, such as in medical equipment, nuclear industry components, and aerospace applications.

Despite its advantages, XPP is a thermoset and is therefore more difficult to process compared to non-crosslinked thermoplastic PP. Thermosets are notoriously difficult to recycle, and this is increasingly a barrier for their use in the modern environmentally-sensitive economy. Recently, the issue of re-processing (recycling, re-purposing) of thermoset plastics has become a topic of intense research, driven by the introduction of “vitriimer” concept.^{2,3} A variety of covalent bond-exchange chemistries have been explored in the last decade, and several complete reviews give sufficient detail of this field development.^{4–6} Here, we are concerned with just one such bond-exchange mechanism, of disulfide bridges.^{7–9} The most common and familiar use of disulfide bridge crosslinkers is in vulcanization of natural rubber,¹⁰ where the bond exchange and the associated creep and stress relaxation have been known for a long time.¹¹ The disulfide exchange has several advantages over many other mechanisms of plastic flow in vitrimers (or otherwise called covalent adaptable networks, CANs¹²): this exchange is catalyst-free, and the activation energy is quite low, ca. 20 kJ/mol depending on chemical environment and chain flexibility, achieving reprocessability in the vitriimer fashion by introducing labile bridges in crosslinkers.^{13–15} This a promising mechanism for higher Melt Flow Index (MFI) in standard plastic processing. In addition, the elemental sulfur (S₈) is quite a cheap commodity material.

As an aside, we would like to clarify the terminology used here. Although for many decades the term “vulcanization” has acquired a broader meaning in the literature, referring to any covalent crosslinking, here we want to exclusively refer to it as “crosslinking by sulfur”¹⁶ as it was initially introduced by Goodyear in 1840s and referred to the volcanic origin of sulfur. It should be noted that unsaturated polyolefins (polyisoprene and polybutadiene) are commonly vulcanized in the rubber industry, and this is not a challenge since the Goodyear times: the vinyl C=C bond is highly reactive in this environment.

Here, we study the classical problem of vulcanization of polypropylene (PP), and by implication, other saturated polyolefins. Early work in the field was done by Dogadkin and Dontsov, who utilized PE in combination with sulfur at high temperature to crosslink them over a long time, drawing parallels to vulcanization of natural rubber.¹⁷ They later briefly characterized the effect of an organic peroxide (dicumyl peroxide [DCP], the same as

we use here) and a popular activator/accelerator pairing (2,2'-dithiobisbenzothiazole/zinc oxide: MBTS/ZnO), widely used in the rubber industry, producing highly crosslinked polyethylene (XPE) products.¹⁸ However, this early work did not exclude the possibility of radically initiated PE crosslinking, a well-known reaction used industrially to produce XPE.^{19,20} Some later work has investigated atactic PP requiring 20 h to produce C=S bonding,²¹ which is of limited use in crosslinking. Finally, to our knowledge, the most recent work has focused on the use of S₈ as a non-reactive filler in PE and PP melts, demonstrating some physical property benefits.^{22,23} Excessive sulfur incorporation has also been studied in the context of conducting plastics,^{24,25} but is not of interest to our work.

Surprisingly, there has been little direct investigation into the peroxide-initiated vulcanization reaction applied to saturated polyolefins for the purpose of their chain crosslinking, meaning the most relevant prior-art case for our work is ethylene-propylene rubber (EPR), where the co-polymer nature prevents chain crystallization and retains elastomeric nature of the material at ambient temperatures. This co-polymer is commonly crosslinked with the aid of peroxides,²⁶ and has been vulcanized when sulfur is added to the system.^{27,28} This and other work has shown that the presence of elemental sulfur reduces the detrimental scission effect common to peroxide treatments of PP.^{29–32} At present, other additives are more commonly used to reduce EPR scission during peroxide-initiated crosslinking in industry,²⁶ but this results in non-labile covalent bonding. Chemically, the saturated EPR system is superficially similar to pure PP, however increasing the PP content in EPR reduces its crosslinking efficiency^{27,33} meaning applying the same peroxide-driven procedure is impossible. Therefore, to vulcanize pure PP a new set of conditions must be explored.

In this article, we explore peroxide-driven radical formation in the high-temperature PP melt in the presence of elemental sulfur, and the resulting crosslinking by sulfide bridges, scanning a range of sulfur and DCP concentrations to cover the evolution from the regime of chain scission at the high-DCP, low-sulfur end to the optimal range of crosslinking, to the regime of re-polymerization at excess sulfur. We characterize the resulting vitriimer plastics, demonstrating a significant enhancement of their mechanical properties at the ambient temperature, and also the ready re-processing with a reasonably high MFI at a high temperature where the elastic–plastic transition is activated. The field of vulcanization of natural rubber is over 100 years old and a lot of tools and additives were introduced to make the products better; notably the effect of accelerators (such as MBTS) and activators (such as ZnO) are extensively discussed in the

literature. In this article, we wanted to stay with as few reacting components as possible and isolate the key effects that control the degree of crosslinking, and the resulting thermal and mechanical characteristics of XPP, so we have given only brief consideration to these additives.

2 | RESULTS AND DISCUSSION

2.1 | Reaction extrusion of XPP

The chemistry of vulcanization of natural rubber has been extensively investigated over the decades, although the mechanism is still debated, and varies with additives.^{34,35} In our system, the dominant expected chemistry is represented in Figure 1A. We first expect the homolytic scission of DCP at 180°C, producing alkoxy radicals represented by R—O*. These radicals initiate a crosslinking mechanism in which tertiary radicals are generated on the PP backbone,³⁶ and rapidly react with elemental sulfur of the S₈ ring, terminating to produce crosslinks with a variable number of sulfur atoms³³ (other products are possible, particularly with higher sulfur concentrations, as reviewed in Reference 25). The β-scission of the PP chain competes with this process,^{29,30} but the presence of reactive sulfur is believed to reduce this, likely by stabilizing the tertiary radicals.^{27,32} Other non-productive termination events are possible, including acidic peroxide decomposition or disproportionation of PP radicals,^{26,36} but they are more likely to reduce the efficiency than fundamentally alter the crosslinking chemistry. Importantly, there are two routes by which non-exchangeable crosslinks can be generated. First, C—C crosslinking can be produced by PP* combinations (though we consider this less likely with high sulfur content due to the instability of tertiary radicals with respect to scission, and the higher mobility of S₈ than PP*). Second, some sources report that at high temperatures, with increasing reaction time, the length of sulfur bridges decreases, eventually producing strong but non-exchanging monosulfidic crosslinks³⁷ as represented at the bottom of Figure 1A.

Considering these mechanisms at play, we examined EPR vulcanization as the closest chemical analogue to our system for initial recipes, where sulfur incorporation has been investigated by extraction and quantification of unattached sulfur. Robinson et al.²⁷ found that a 4:1 DCP:S ratio gave the optimal incorporation, while Moore and Trego found that a 10:1 DCP:S ratio gave good incorporation with monosulfidic crosslinking, and 2:1 DCP:S gave less efficient incorporation of sulfur with a higher proportion of polysulfidic links.²⁸ Thus the literature suggests an optimal ratio of initiator and sulfur exists in

saturated systems for incorporation. Below this ratio, low incorporation may result because there are not sufficient radicals (as termination consumes radicals). The reduction in crosslinking below this ratio may be enhanced by a mechanism in which excess sulfur at high temperature can degrade the existing sulfur crosslinks, as reported in the early literature.¹⁸ In our system, degradation of PP may also result from sulfur radicals generated by polymerization of sulfur above 159°C,^{38,39} which is likely to have a larger effect with more free sulfur. Above this ratio in EPR systems we might expect that all sulfur would be incorporated so limited benefit would be derived, except from additional C—C crosslinking.

To investigate this initiator/sulfur relationship in our system, we performed this reaction using a twin-screw compounder at 180°C to melt PP and mix the components under high shear. Figure 1B illustrates the rheological signature of this process, presenting the chamber pressure in the compounder. This plot presents the series of reaction-extrusion tests with the data cleaned from a variety of artifacts (the raw data is presented in the Supporting Information, e.g., Figure S1d for this particular loading of 10 wt % S). One important element is the alignment of the time axis for all the curves, which makes it easier to track the key points. There are three key points marked by arrows in this plot: (A) on the initial loading of the PP + S₈ mix, the melt quickly reaches an equilibrium showing as a plateau pressure. The difference between the curves is because we needed to have the total chamber load of 5 g, and with the higher DCP content, there was proportionally less PP + S₈ loading, and so lower pressure reading. Point (B): when the measured amount of DCP was added (in small aliquots to help more homogeneous initiation in the sample volume), the pressure rapidly increased, indicating crosslinking (with the accompanying disulfide bond exchange allowing plastic flow to continue), before finally saturating at a final value of vitrimer pressure, increasing with increasing DCP content. Point (C): at very high DCP loading, we find the prominent pressure oscillations, which we associate with non-uniform crosslinking (the higher crosslinking density zone, where the DCP was initially inserted, travels around the compounder passing the pressure sensor periodically). This being the bond-exchanging vitrimer, we expect the network would eventually homogenize. However, we were not comfortable leaving the reaction in the hot high-shear compounder for over an hour, and extruded those materials—later finding that the ductility of their samples was much lower than of those that reached a homogeneous crosslinking and a clear pressure plateau reflecting the constant “melt viscosity” or MFI (it is not a melt, but the plastically deforming vitrimer at this stage).

This was repeated for a range of different sulfur concentrations, producing the characteristic traces of time

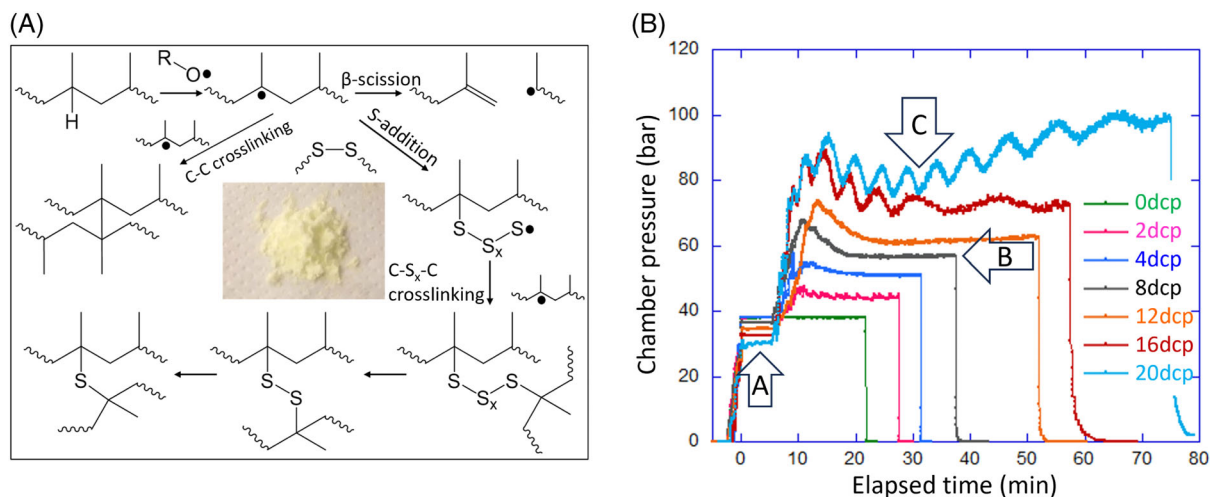


FIGURE 1 Vulcanization of PP: (A) the chemistry of processes going clockwise from top left, with the side C–C crosslinking reaction. The central photo illustrates the S₈ elemental sulfur. R–O* represents a DCP-derived radical. (B) The example of evolution of chamber pressure during reaction in the melt compounder at 180°C: initially the PP mixed with S₈ are loaded and the melt flow equilibrated (point A), then the labeled amount of DCP is added and the dynamic crosslinking takes place (point C), before extruding the plastic (point B, all discussed in the text).

evolution of chamber pressure, from the initial loading to the final extrusion (see Supporting Information). The data could be summarized, and usefully interpreted, if we plot the final pressure in the vitrimer plastic, just before the extrusion, against the composition, in Figure 2. This final pressure is directly related to the melt flow index (MFI), broadly used in plastics industry: Supporting Information gives the details of this calculation, but for the standard ASTM D1238 definition of MFI 230°C, the melt viscosity in SI units is $\sim 10/\text{MFI}$, so for the MFI = 34 for our PP3950, its viscosity would be ~ 0.3 Pa s and the compounder chamber pressure is linearly proportional to it. The results show the MFI dropping to 13–15 in our higher-crosslinked XPP samples, which is still well within industrial processing margins.

The scission effect of DCP is fast and prominent in sulfur-free PP, as the curve with 0S indicates in both plots in Figure 2, where the chamber pressure (and so the melt viscosity) rapidly drops to zero. In PP-S mixtures, below a threshold DCP:S ratio the peroxide addition leads to a marked pressure increase, while above this threshold a decrease in pressure due to chain scission is observed (we only captured two of these maxima in the 0.5% and 1% S systems, because our experiment [nor the common sense] did not allow adding excessive amounts of DCP). This suggests sulfur buffers the scission effect of DCP until it is fully consumed by an approximate 8:1 DCP:S weight ratio, consistent with the literature on incorporation in EPR,^{27,28} and also the estimate reported by Reference 33. This also corresponds to a simple count, that at the maximal crosslinking, each sulfur atom accounts for

two DCP radicals, so in an ideal reaction every sulfur atom would form a monosulfide link. Clearly the actual chemistry is more diverse, as the material can still be reprocessed, meaning there are many disulfide bridges to exchange. Part of this deficiency likely stems from alternative termination reactions such as disproportionation and C–C crosslinking, but it is important to note that this DCP:S ratio is likely to be an overestimate. The real maximal ratio is likely to be lower than 8:1, as the loading of DCP at 180°C is associated with some evaporation loss, which we could not control.

There are other known routes of non-homolytic DCP degradation: aerobic degradation (in spite of our use of nitrogen flow in the compounder), the reaction between sulfur and DCP,²⁷ or the acidic decomposition of DCP, which is often addressed by the inclusion of ZnO “activator.”²⁶ In the end, the net effect of DCP degradation may be significant in this reaction-extrusion process of PP vulcanization.

As a result, we have produced series of compounds with no sulfur at all, with 0.5, 2, 5, and 10 wt% S, which we label for brevity as samples 0S, 0.5S, 2S, 5S, and 10S, respectively. The same labeling convention was used for the DCP content, so a sample with 5 wt% sulfur and 12 wt% DCP is labeled as 5S-12DCP.

As an aside, accelerators and activators are widely used in the rubber industry to control the rate of vulcanization, though the mechanisms are only partially understood.^{34,40} Seeking to apply some of these benefits to our system, we tested accelerator and activator additives individually. The base ZnO is commonly used in peroxide

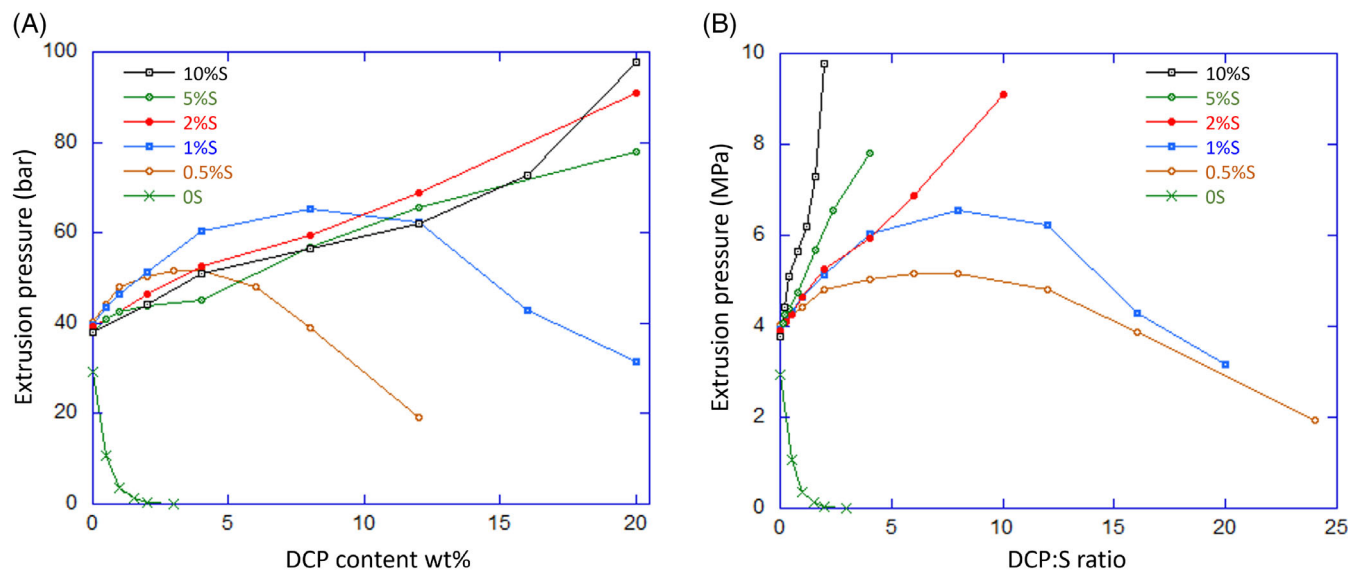


FIGURE 2 Melt-flow pressure for different S and DCP content: (A) plotted against DCP content, for several sulfur concentrations; (B) the same data plotted against the DCP:S weight ratio. In both cases, the competition of DCP-induced chain scission and S-induced dynamic crosslinking is apparent.

systems to mitigate acidic hydrolytic decay of peroxide,²⁶ so we tested 5 wt% ZnO with 5S and 4, 8 or 12DCP but observed no difference in physical properties. The accelerator MBTS has been claimed to crosslink PE with only S₈ present,¹⁸ replacing the radical initiation by peroxide. Therefore, we attempted to replicate this report using PP, but the products were clearly uncrosslinked over the course of a 2-h compounding. Given these negative results (details in the Supporting Information), we decided to focus on the pure PP-S-DCP system to further investigate vulcanization in this work.

2.2 | Evidence of crosslinking

One important, but indirect evidence of PP crosslinking by sulfur vulcanization is the significant increase in the compounding pressure discussed above. We applied Raman spectroscopy trying to gain direct evidence of such covalent bridging. Raman spectra were acquired for the series of compounds with 0S, 0.5S, 2S, and 5S (see Supporting Information for detail). No direct evidence for C—S bonds was observed. This is unsurprising as such peaks are usually extremely weak.³⁴ Remaining Raman peaks were entirely attributable to isotactic PP,⁴¹ with the exception of a 475 cm⁻¹ peak, which is likely due to S—S stretching in the elemental sulfur S₈ ring.²³ Tracking the area of this peak, normalized to the nearby 398 cm⁻¹ peak known to correspond to ω CH₂ + δ CH stretch,⁴¹ showed the magnitude increased with increasing of sulfur loading, as expected—but decreased with increasing DCP concentration,

consistent with the consumption of S₈ rings in crosslinking. This is also supported by the absence of any other sulfur peaks, such as S—H stretching at 2570 cm⁻¹,^{42,43} indicating no side reactions. Finally, the absence of non-PP peaks in the region 950–1200 cm⁻¹⁴⁴ means that DCP could not be identified, even when 20 wt% was added. This is consistent with the loss of volatile degradation products of DCP,⁴⁵ meaning in our system DCP residuals are unlikely to impact the extruded material.

The other common crosslinking characterization method is the gel fraction. In previous studies of PP-based vitrimers, crosslinked with bonds exchanging by transesterification⁴⁶ or thio-ester exchange⁴⁷ (both a much lower rate of exchange), measuring the gel fraction measurement after swelling the vitrimers in hot xylene was returning high values of 55%–60%, confirming the insoluble covalently crosslinked network. However, repeating the same procedure in our vulcanized PP vitrimers has returned an unexpected result. Even though the highly crosslinked systems are very obviously rubbery at high temperature (not melting but displaying an elastic bounce), there was no resistance to xylene at high temperatures, even in some of the most heavily crosslinked plastics (5S-12DCP, 10S-20DCP, and 2S-8DCP). We will find several similar results in other tests, all pointing to the fact that the disulfide bridges have a rather high rate of exchange, and this apparently allows the network to creep and eventually to dissociate under the swelling pressure. See the earlier study (for transesterification) where it was demonstrated that swelling initiates bond exchange, by mechanochemically shifting the activation energy.⁴⁸

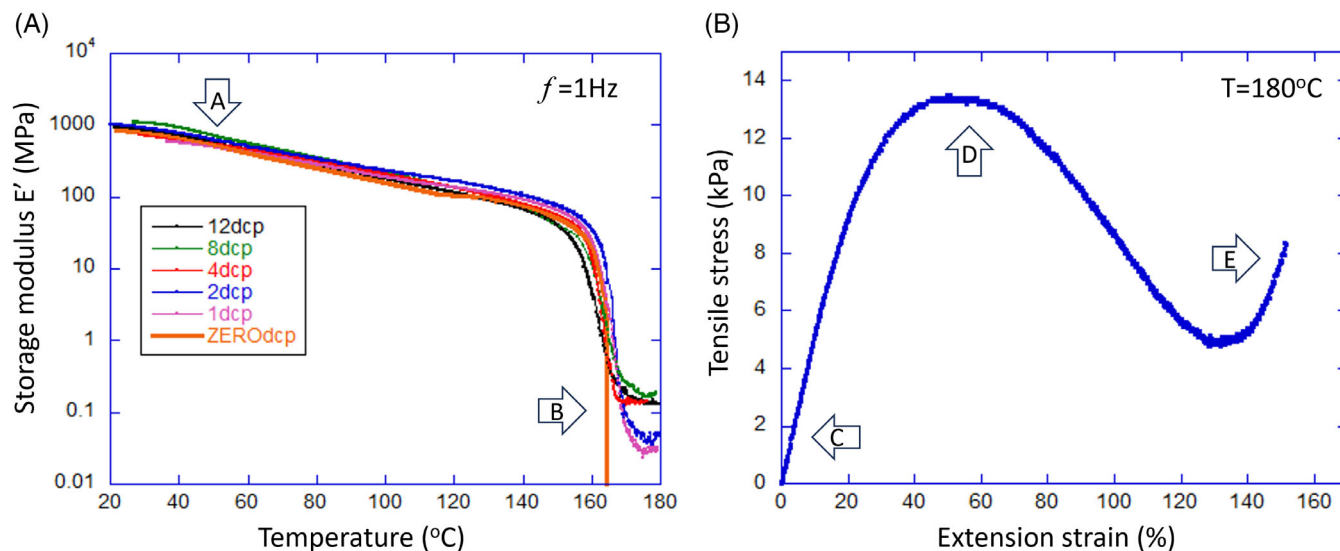


FIGURE 3 Mechanical response at high-T. (A) The DMA temperature ramp, in tensile mode, of a series of XPP with 5S and increasing loading of DCP (with the proportional increase in crosslinking density). The uncrosslinked melt (zero DCP) melts at $T_m = 165^{\circ}\text{C}$. The onset of the rubber plateau is evident on increasing of DCP. Points (A) and (B) are discussed in the text. (B) The stress–strain tensile test of XPP (5S-12DCP) in the “rubber-elastic” regime at 180°C and constant strain rate of 0.002 s^{-1} . The initial rubber modulus (point C in the plot) soon turns to the yield stress turning (point D in the plot), followed by the plastic flow. However, at the high deformation there is a new stress increase (point E in the plot), indicating a small fraction of permanent crosslinks.

What else could we test to quantitatively confirm the covalent network crosslinking in our XPP? One may hope to identify the rubber plateau modulus in a dynamic-mechanical test at high temperature. Figure 3A shows several DMA scans in the linear tensile regime, at a constant 1 Hz oscillating strain (of 0.1%), on increasing temperature. At ambient temperature, all plastics show the very similar Young modulus: point (A) in the plot. On heating they all undergo the melting transition around $T_m = 165^{\circ}\text{C}$. The reference PP3950 plastic melts into a viscous fluid, but the crosslinked XPP samples all show an onset of a rubber plateau, at a different level clearly dependent on the effective crosslinking density: point (B) in the plot. However, we were not able to extend the test to higher temperatures because all samples have plastically flowed to the maximal length of the instrument. We, therefore, conclude that there is a solid evidence of crosslinking, yet the high-temperature rubber-elastic regime is not easy to work with because the relatively high rate of disulfide bond exchange makes these “rubbers” plastically deformable (see Supporting Information for further data). In the end, this is actually an advantage, because it does allow a much higher Melt Flow Index and easier re-processing of these vitrimers, while their practical use is mostly at the ambient temperatures.

Figure 3B presents a different angle on the mechanical properties of XPP. Normally, a crosslinked thermoset would display the classical rubber elasticity when well above its glass or melting transition. We therefore carried

out stress–strain tensile tests at $T = 180^{\circ}\text{C}$, expecting to measure the rubber modulus and thus assess the crosslinking density. Figure 3B shows such a stress–strain curve for a densely crosslinked (5S-12DCP) XPP sample, at a very low strain rate, which permits estimation of the rubber modulus: point (C) in the plot, giving $G = E/3 \approx 20\text{ kPa}$ (in the incompressible rubbery regime). This is slightly lower than the Young modulus suggested in the oscillating test in plot (A), but that was measured at strain rates almost 1000 times higher.

The prominent transition to plastic flow past the yield stress (point D in the plot) turns out to reveal the true nature of bond exchange. The earlier study of elastic–plastic transition in vitrimers⁴⁹ has discussed this test scenario and derived the time-dependent expression for the measured stress, which depends on just two parameters: the equilibrium rubber modulus G and the rate of bond exchange β ,

$$\frac{\sigma(t)}{G} = e^{-\beta t} \left(\lambda(t) - \frac{1}{\lambda(t)^2} \right) + \int_0^t e^{-\beta(t-t')} \left(\frac{\lambda(t)}{\lambda(t')^2} - \frac{\lambda(t')}{\lambda(t)^2} \right) \beta dt, \quad (1)$$

where the tensile strain is $\lambda = 1 + \dot{\epsilon}t$ at the applied constant rate $\dot{\epsilon}$. For a larger strain (or time of experiment, for the constant strain rate $\dot{\epsilon}$) the stress would reach a maximum (yield point) after which the material would carry on with the plastic flow. According to the theory, the

yield stress occurs approximately when $\beta t = 1$, which for our strain rate implies the rate of bond exchange $\beta = 3 \times 10^{-3} \text{ s}^{-1}$ for the strain point of ca. 60%. Interestingly, the final rise in stress at very large strain (point E in the plot) is also captured by the theory⁴⁹: it is a consequence of a small fraction of permanent crosslinks in what was dubbed “partial vitrimers.” We have discussed above the low probability of direct C—C chain crosslinking, and also monosulfide bonds, that could occur in our organic peroxide initiated process, and produce this stiffening effect.

2.3 | Thermal properties

Calorimetry was used to assess the melting temperatures and enthalpies of our samples. Figure 4 illustrates the melting phase transition in several selected compositions of our XPP vitrimers. The two base scans, of the S_8 , and of our pure PP, are compared with the melting transitions when additives are present. The first three curves have only S_8 , and no DCP, and so there is no crosslinking, the sulfur just playing the role of impurity. Remarkably (also see the numerical data in Table 1), there is practically no change in the melting point or the degree of crystallinity, up to our highest 10 wt% of sulfur. This indicates that the impurity is expelled from the crystalline regions into the amorphous zone of PP during the nucleation and growth stage of the transition: an effect known in many other first-order phase transition systems with impurities.

Examining the melting transition of the crosslinked (vulcanized) PP networks, we again see little change comparing with the base PP. As with 0DCP plastics, there is no trace of sulfur transitions, that is, no phase separation occurs even on a small scale. There could be a small shift of the melting point to lower temperatures with the increase of dopant concentration, but this is a small effect certainly not relevant in any practical use of the modified plastic.

Fraction of crystallinity (or the degree of crystallinity) was calculated by taking the ratio of latent heat against the theoretical value for the fully crystalline PP: ΔH_0 is 207.0 J/g.⁵⁰ The base PP3950 has about 40% crystallinity, and Table 1 shows how this fraction decreases slightly with the increasing sulfur concentration: whether covalently bonded into bridging crosslinks, or unreacted sulfur remaining in the plastic. A minor effect of unreacted sulfur lowering crystallinity has been previously observed, and speculated to derive from an effect of elemental sulfur on crystallization.²³

The tabulated data for samples with 0S, and increasing DCP, illustrates the chain scission (also seen in Figure 2), with the associated decrease of crystallinity.⁵¹ The effect of increasing DCP with sulfur present, to react

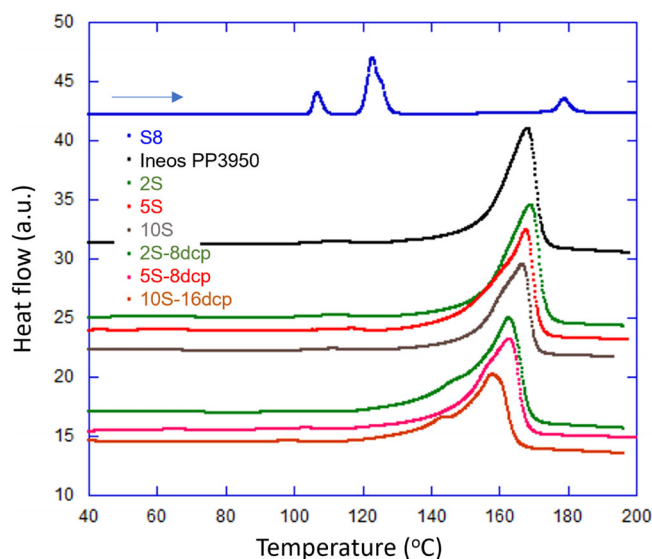


FIGURE 4 Differential calorimetry scans illustrate the melting phase transition on heating. The scan of pure S_8 shows several transitions, in agreement with the literature data; none of these are visible in the XPP scans even at 10S. The melting of semicrystalline PP3950 confirms the literature value of $T_m = 165^\circ\text{C}$. Several scans of XPP with 2S, 5S, and 10S, without and with DCP, show little change in this melting transition.

with the created radicals and protect PP chains from scission (see the extended discussion around Figure 2), is to increase the crosslinking by sulfide bridges. The degree of crystallinity apparently falls with increasing crosslinking as well.

2.4 | Mechanical properties at ambient temperature

Most of the practical uses of rigid semi-crystalline plastics, such as PP, are at the ambient temperature well below their melting point. Therefore, the fact that PP is covalently crosslinked may not have a strong effect on the mechanical properties. The key test of these properties for a rigid plastic is the tensile test to break, using either the ASTM D638 or the ISO 527 standards. Fundamentally, both test the same characteristics, and we followed the ASTM D638 protocol.

Figure 5 illustrates the effect of PP vulcanization on the example of 5S XPP compositions. The tensile test of the base PP returns the values closely matching the Ineos PP3950 datasheet: the Young modulus $E \approx 200$ MPa, yield stress ca. 25 MPa, elongation to break ca. 130%. Adding sulfur without DCP merely creates impurity in the plastic, and slightly diminishes the yield stress. Point (A) in the plot illustrates the fact that the linear (Young) modulus is almost the same in all materials: we understand

TABLE 1 Degree of crystallinity in vulcanized XPP.

wt% S-wt% DCP	ΔH (J/g)	Crystallinity (%)	Shore D	wt% S-wt% DCP	ΔH (J/g)	Crystallinity (%)	Shore D
0S-0DCP	89.8	40	68	5S-0DCP	82.6	40	66
0S-0.5DCP	81.7	36	68	5S-1DCP	78.5	38	67
0S-3DCP	71.1	32	65	5S-4DCP	73.8	36	67
0S-12DCP	48.7	22	63	5S-8DCP	69	33	69
0.5S-0DCP	86.5	41	68	5S-12DCP	64	30.9	70
0.5S-1DCP	80.1	39	68	5S-20DCP	59.2	29	69
0.5S-4DCP	71.7	35	67	10S-0DCP	74	36	63
0.5S-12DCP	52.8	26	66	10S-1DCP	72	35	64
2S-0DCP	85.5	41	66	10S-4DCP	69.2	33	65
2S-1DCP	77.9	38	68	10S-8DCP	66.5	32	65
2S-4DCP	72.6	35	69	10S-12DCP	64.4	31	68
2S-8DCP	67.3	33	69	10S-16DCP	62	30	67
2S-12DCP	63.4	31	69	10S-20DCP	60.8	29	67

Note: Enthalpy (latent heat) of the melting transition in XPP materials (with an error ca. ± 1 J/g), and their corresponding degree of crystallinity estimate. The 0S-0DCP sample is the initial standard Ineos PP3950. The error in the crystallinity estimate was $\pm 1\%$ – 2% . The error in the durometer measurement of plastic hardness was ± 1 (Shore D scale, see the discussion in Section 2.4).

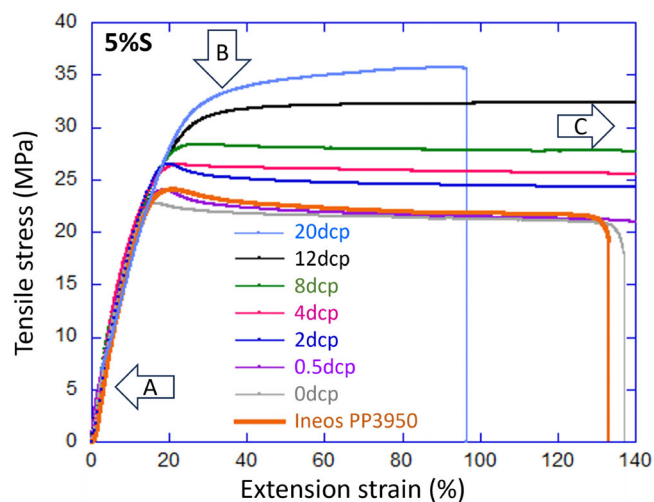


FIGURE 5 Tensile tests of crosslinked plastics. The ASTM D638 stress–strain curves for the range of samples with 5S, and increasing DCP content (as labeled in the graph). Points A, B, and C highlight the linear (Young) modulus, the ultimate (yield) stress, and the strain to break (ductility), respectively.

this is because this modulus is determined by the composite nature of semicrystalline plastic at room temperature. In addition, the Shore Hardness data presented in Table 1 delivers a very similar message: the linear modulus of all XPP materials is very similar to that of the original PP (which is listed in its technical datasheets). However, there are noticeable deviations in Shore Hardness (above the test uncertainty): down to 63 for highly

disrupted 0S-12DCP and 10S-0DCP networks, and up to 70 in the “optimally crosslinked” 2S-8DCP and 5S-12DCP networks.

We see a marked increase in mechanical strength on the increasing XPP crosslinking (point B in the plot). This trend is reproduced at all sulfur loadings we tested: 10S, 2S, even 0.5S but with a lower effect (see Supporting Information for the full data). It is also important to note the changing nature of plastic deformation: the zero/low crosslinking density results in a pronounced necking and the stress decrease past the yield point, a well-studied effect in rigid thermoplastics. In contrast, with more substantial crosslinking, we see no such sharp necking, but instead a more gradual transition to plastic deformation. In this regime, we also find the remarkable increase in plastic ductility (point C in the plot), which is emphasized in Figure 6A. At a high crosslinking density, the ductility diminishes (as expected), while the ultimate stress becomes much higher than in the base PP.

We attribute this remarkable and unexpected ductility to the exchangeable nature of sulfur bridges. Although the rate of spontaneous exchange must be very low at the ambient temperature, the high natural lability of disulfide makes it activate mechanochemically, at the high tension of chains at large deformation. This could serve to blunt, and ultimately self-heal the cracks that would lead to the break of the base PP. Such re-connecting chains must be the origin of such an enormous ductility. This would not be found in an ordinary weakly crosslinked PP, without bond exchange. Naturally, this

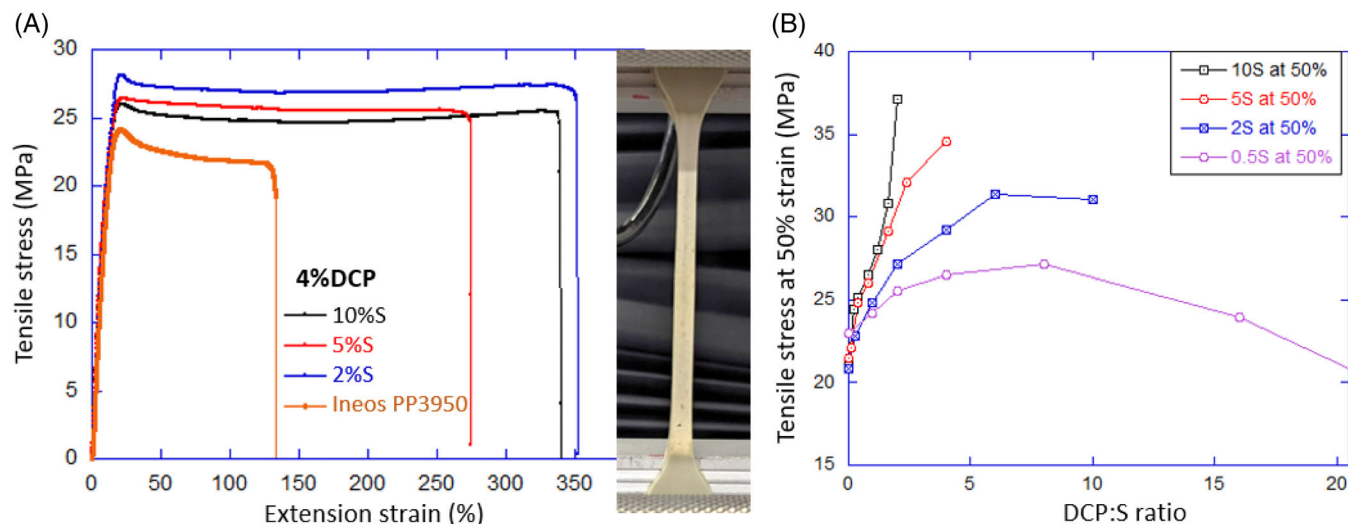


FIGURE 6 Strength and ductility of XPP. (A) The tensile stress–strain test shows the enormous ductility of XPP plastics with different S-content, all at 4DCP, compared with the standard base PP. The image illustrates the changes in the material morphology on such a high plastic elongation. (B) The summary of mechanical strength, showing the tensile stress at 50% elongation (well past the yield point) against the DCP:S ratio in the composition.

“self-healing” effect competes with the increasing chain tension in a more densely crosslinked network, and in those XPP samples the elongation to break diminishes (still, a 80%–100% strain to break is far from a “brittle” plastic, see Figure 5 and Supporting Information). It should be noted that sulfur alone has been shown to increase the ductility of polypropylene, but the magnitude of this effect increases dramatically above 5S,²³ meaning in our case it is only likely to have had an effect in 10S samples, where it may be the majority of the ductility effect given the low expected crosslinking with such low DCP:S ratios.

Figure 6B summarizes the tensile stress–strain data in a representation similar to that of Figure 2B, plotting the stress against the DCP:S composition ratio. The discussion of chemical reactions in the material has suggested that this ratio has an optimal value, at which the crosslinking is maximally efficient. Our experimental composition window did not allow us to capture this maximum point for 10S and 5S, and only just for the 2S, but the trends appear to be convincing. Below this optimal ratio, crosslinking may be inefficient due to the reasons discussed in Section 2.1, and additionally mechanical properties could be altered by excess dissolved sulfur disrupting PP crystallinity/structure.²³ At and above this ratio we do not observe thermoset properties in our materials, which suggests that even if complete sulfur incorporation with monosulfide crosslinks can be achieved in PP, under our conditions the effect of scission from PP* in the absence of sulfur cancels any benefit in physical properties. Thus our maximum ratio for improved

physical properties, around 8:1 DCP:S (which is likely an overestimate as discussed in Section 2.1), reflects the prevalence of di- and polysulfide linkages in the absence of high scission and excess free sulfur.

2.5 | Vitrimer features: re-processability and welding

The main purpose of this paper is to demonstrate, and explore the conditions for the vulcanization of a structural commodity plastic: polypropylene. However, there are two remarkable properties, unique to vitrimers, which we also need to highlight in the XPP system here. The first of these is the repeatable reprocessability. There is nothing remarkable in multiple reprocessability of thermoplastic, but the ability of a covalently crosslinked network to retain its key properties after multiple session of stress-induced plastic flow (either in compounder or in injection molder) is the biggest selling point of vitrimers, especially in the present environmentally-sensitive public mood. We found that vulcanized XPP is performing much better in this respect, comparing to many other vitrimers in the literature. We find almost no degradation when the first re-processing is done over minutes in the twin-screw compounder at 180°C, or over seconds in the injection molder at 200°C. Figure 7A compares the key ASTM D638 tensile test of two example materials, 5S-4DCP and 5S-12DCP: freshly-made (labeled “rep1”) and after several cycles of complete remolding (the plot legend lists “rep2,” “rep3,” and “rep5” for the number of complete re-processing times). The freshly-

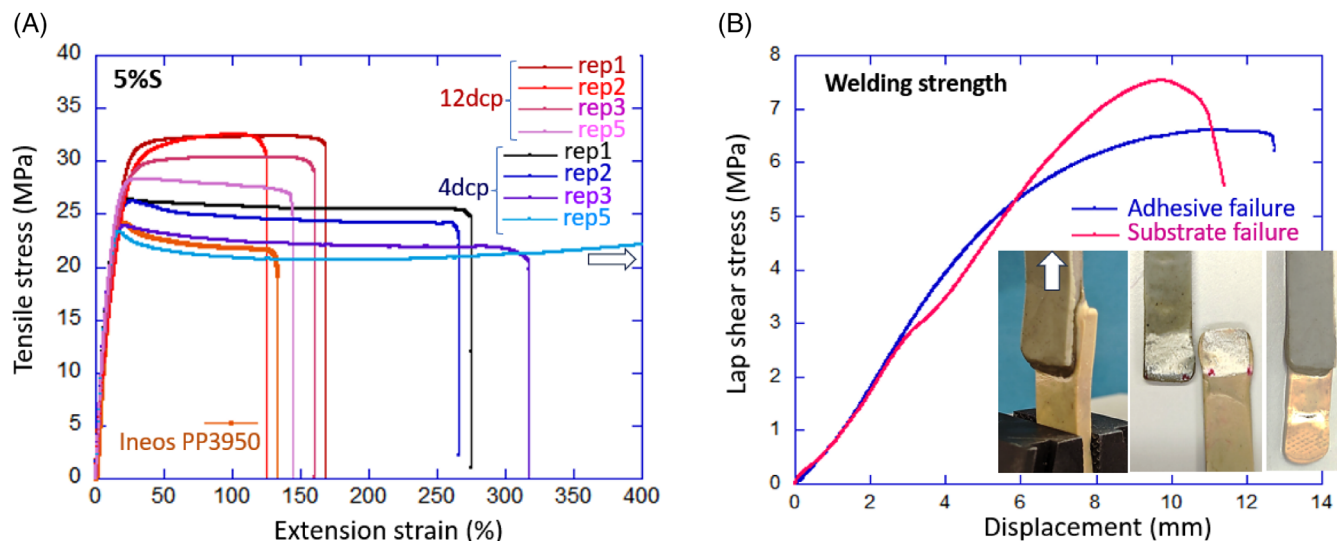


FIGURE 7 Reprocessability and welding strength. (A) The tensile stress–strain test shows the enormous ductility of XPP plastics with different S-content, all at 4DCP, compared with the standard base PP. The image illustrates the changes in the material morphology on such a high plastic elongation. (B) The summary of mechanical strength, showing the tensile stress at 50% elongation (well past the yield point) against the DCP:S ratio in the composition.

made curves are those already present in Figure 5, and the original thermoplastic PP3950 is also shown for comparison. The mechanical properties (hardness, modulus, and yield stress) are almost un-changed after the first re-processing, but on the increasing number of chopping and injection-molding cycles the gradual downward drift of mechanical properties is found. Clearly, the XPP material remains viable, but some degree of network degradation does occur. The variation in strain to break (ductility) is most strongly affected by the re-molding conditions (which we could not maintain 100% constant), leading to a slight difference in crack nucleation on the dogbone edge; however, the 5-times reprocessed 5S-4DCP plastic has shown an enormous ductility (we stopped the test at 600% strain, still not broken): the crack-healing mechanism is clearly retained even in spite of some network degradation.

As an aside, high temperature (230°C in the ASTM D1238 standard procedure) reprocessing of samples for MFI calculation also showed some degradation of their physical properties (data not shown). At this high temperature, the presence of sulfur radicals is much enhanced,³⁸ and the degradation effect from excess sulfur attacking existing crosslinks is certainly present.¹⁸ Indeed we found that reprocessing at 230°C results in a continuous decrease in MFI as well (see Supporting Information). Higher temperatures also favor the radical initiated degradation of PP*.⁵² Therefore we consider that the lowest possible temperature is likely optimal for processing (and recycling) these materials.

The second remarkable feature of vitrimers is their direct welding ability. Unlike metals, welding of polymers

is a notoriously difficult proposition. It certainly cannot occur in thermosets, and is very poor in thermoplastics because to interpenetrate, the locally molten chains need to follow a very long reptation process. Vitrimers, due to their bond exchange across interface (even when different plastics are in contact) allow covalent bonding without the need for chains to reptate into the material opposite.^{3,47,53} The ready, catalyst-free disulfide exchange is expected to facilitate a particularly good welding.

We demonstrated welding by joining two different vulcanized XPPs: 5S-4DCP and 5S-12DCP. Without an extensive (and necessary) optimization of conditions, we welded these two plastics using a surface flashing temperature of 200°C (measured crudely by a thermal imaging camera) for 5–10 s, and then holding two surfaces together by finger pressure for 20–30 s, till the contact temperature drops below the melting point. The welded plates were tested for lap shear stress (ASTM D5868 test standard), demonstrating strong bonding, see Figure 7B. In many cases, the substrate failure occurred instead of debonding, as illustrated in the inset images. Importantly, the lap shear strength of welding reaching 6–7 MPa is very high by industry standards.

3 | CONCLUSIONS

We have demonstrated a successful vulcanization process of standard isotactic polypropylene, that is, formation of covalent sulfide bridges between saturated aliphatic chains via radical initiation. A range of compositions,

including the sulfur and peroxide content, as well as the effect of industry-standard activators and accelerators, were investigated, and clear optimization “sweet spots” were identified. With these optimal compositions, cross-linked XPP has a much enhanced mechanical properties in the ambient state of rigid plastic, and high thermal stability (i.e., not melting but turning into a plastic rubber).

However, we were not able to explicitly demonstrate the “rubber plateau” of our dynamic XPP at high temperatures. Neither oscillating DMA test, nor static iso-stress results, show the classical rubber elasticity when the material is high above its melting temperature. Instead, both these tests show a clear plastic flow: not the simple viscous flow as in the molten PP, but the typical plastic creep of vitrimers.⁵⁴ It is clear that we observe a trade-off: due to crosslinking with easily exchangeable sulfide bridges, at the high temperature required to melt the semi-crystalline polypropylene the network is already well in the plastic-flow regime and not letting us see the pronounced rubber plateau. It is actually the same with most vitrimers we know about in the literature: the desire to have the bond exchange and the elastic–plastic transition at an elevated temperature, with a practically reasonable Melt Flow Index, prevents the clean regime of rubber elasticity.

The main example of the opposite: of the well identified rubber-elastic regime at low temperature and the plastic-creep regime at a high temperature, would be the vulcanized natural rubber. The unsaturated flexible chain of polyisoprene or polybutadiene prevents their crystallization and gives a very low glass transition temperature.¹⁶ Vulcanization of such rubber produces a homogeneous rubbery network, which greatly enhances its physical properties. However, such networks are very challenging to reprocess, which is a key distinction from our system. Reprocessing by heat treatment has been attempted for natural rubber, but suffers from scission at high temperature and is argued to generate non-exchangeable monosulfide links limiting the repeatability.^{55,56}

Our work had a focus on vulcanization of rigid polyolefin plastic (such as the saturated isotactic polypropylene) to impart enhanced thermal stability, improve mechanical properties, and also add the welding capability as with all vitrimers.^{46,57} Vulcanization of other saturated polyolefins is theoretically possible as all have the same C–H bond, which we exploited in polypropylene. However, there are important differences in base radical reactivity meaning the reaction needs a separate tuning in other systems. For example, in PE, crosslinking is favored over scission, which means that high temperature conditions do not lead to scission (as we had in PP) and may facilitate sulfur crosslinking even without peroxide initiation.¹⁷ On the other hand, in polystyrene, the

literature suggests scission is predominant at tertiary backbone radicals,⁵⁸ and that mixing with sulfur at high temperature reduces overall molecular weight.⁵⁹ Thus, similar to PP, the more stable C* may facilitate scission suggesting that gentle conditions may be required. More reactive polymers require additional considerations—for instance, the terminal amine groups in nylon are thought to react with sulfur,⁶⁰ which could impede crosslinking. If these hurdles can be overcome, this vulcanization reaction would represent a facile way to modify all or most saturated hydrocarbons, with potential to aid reprocessing of mixed waste by crosslinking between species. Therefore, the remaining tasks, and attractive questions, are to achieve this vulcanization crosslinking in other commodity plastics, and in their blends, aiming to produce the next generation of truly re-processable plastics from the recycling feedstocks.

4 | EXPERIMENTAL SECTION

4.1 | Materials

There are many different kinds and varieties of polypropylene, and here we have used the common isotactic “Impact Polypropylene” PP3950 produced by Ineos. Elemental sulfur (S₈), dicumyl peroxide (DCP), the “accelerator” 2,2′-dithiobisbenzothiazole (MBTS), the “activator” zinc oxide (ZnO), and the solvent xylene were all purchased from Merck Sigma Aldrich.

4.2 | Reaction extrusion

The mixing, crosslinking, and extrusion of XPP was carried out in the 7 cm³ conical twin-screw compounder HAAKE MiniLab 3 (ThermoFisher) with an integrated recirculation channel under continuous nitrogen flow. The recirculation was essential to allow the sufficient reaction time, before switching to extrusion of the final material. We found the suitable process conditions at 180°C and 100 rpm screw speed, monitoring the pressure of the melt at two points along the recirculation channel (which gives direct information about the effective viscosity, and allows to calculate/predict the Melt Flow Index).

The process involved first measuring the weights of all compounds such that the total did not exceed 6 g, see the discussion about Figure 1B, then mixing the PP pellets and sulfur (with ZnO or other activator agents, if relevant) and loading it into the compounder. After a pressure plateau was established, indicating full melting and mixing, we added the peroxide in several small aliquots to ensure more homogeneous introduction of

radicals in the melt volume. After that, we allowed the reaction to proceed to full homogenization, indicated by the stable pressure plateau, and extruded the product into a filament.

4.3 | Post-crosslinking processing

The extruded plastic was loaded into the HAAKE Injection Moulder IM4 (ThermoFisher) to inject standard plastic dogbones for ASTM D638 tensile testing. We found the suitable process conditions at 200°C and 300–450 bar pressure (increasing for higher crosslinking density, leading to lower Melt Flow Index of the material).

Other tests (spectroscopy and DMA) required thinner plates of the plastic, and these were produced by hot pressing between parallel plates at 180°C, for 3–5 min. In spite of the evident crosslinked nature of the plastics, most obvious by its “rubbery” feel and elastic bounce at high temperature, the S–S bond exchange allowed complete homogenization of plastic pieces; for instance, after tensile test, the broken pieces of dogbones were re-loaded into the injection molder and re-injected, with properties not visibly degrading after over five times of such reprocessing.

4.4 | Mechanical and thermal testing

All samples were tested in differential calorimetry (DSC4000 from Perkin Elmer) to verify the PP melting and the fraction of crystallinity obtained from the enthalpy of the melting transition. Stress strain tensile tests to break (ASTM D638) were performed on the Tinius Olsen ST1 dynamometer. Dynamic-mechanical characterization was performed on the DMA 850 from TA Instruments, in two modes: the temperature ramp in the linear oscillating regime at a fixed 1 Hz, and the isostress test with the sample heated while loaded with a constant low stress (of 50 kPa)—in both cases to monitor the transition from semicrystalline rigid plastic to the melt/rubber above 160°C. The Shore D hardness was measured directly with a standard Shore D Durometer, at room temperature.

4.5 | Spectroscopy

It was difficult to monitor the reaction conversion of elemental sulfur into crosslinks, because the characteristic vibration modes of the S–S and the C–S bonds are at 400–500 and 600–700 cm⁻¹ respectively,⁶¹ which is outside the range of a standard FTIR spectroscopy (we have

seen no difference in the IR spectra in the Thermo Scientific Nicolet iS10 spectrometer between the base PP3950 and all of our XPP plastics). Therefore we produced Raman spectra with the Renishaw inVia Reflex Raman Spectroscopy Microscope with a 785 nm excitation laser, 10 s integration time and 5% laser power. Data was processed in OriginPro (Origin Lab).

4.6 | Gel fraction

Gel fraction was attempted by submerging PP/XPP (0.2 g) from dogbones in xylene (50 mL) for 48 h. Samples were held at 180°C, at which temperature no samples (including pure PP3950) dissolved, or 190°C, at which temperature all samples dissolved.

ACKNOWLEDGMENTS

This work was supported by the European Research Council (H2020) AdG “Active Polymers for Renewable Functional Actuators” No. 786659. M.O.S. acknowledges the support of The Royal Society University Fellowship. We are grateful to Magna International Corporate Research for providing us the standard polypropylene (Ineos Impact PP 3950) in sufficient quantity for this study.

ORCID

Eugene M. Terentjev  <https://orcid.org/0000-0003-3517-6578>

REFERENCES

- [1] W. Kaminsky, *Macromol. Chem. Phys.* **2008**, *209*, 459.
- [2] D. Montarnal, M. Capelot, F. Tournilhac, L. Leibler, *Science* **2011**, *334*, 965.
- [3] M. Röttger, T. Domenech, R. van der Weegen, A. Breuillac, R. Nicolay, L. Leibler, *Science* **2017**, *356*, 62.
- [4] W. Denissen, J. M. Winne, F. E. Du Prez, *Chem. Sci.* **2016**, *7*, 30.
- [5] S. Wang, M. W. Urban, *Nat. Rev. Mater.* **2020**, *5*, 562.
- [6] C. Bowman, F. Du Prez, J. Kalow, *Polym. Chem.* **2020**, *11*, 5295.
- [7] Z. Q. Lei, H. P. Xiang, Y. J. Yuan, M. Z. Rong, M. Q. Zhang, *Chem. Mater.* **2014**, *26*, 2038.
- [8] F. Zhou, Z. Guo, W. Wang, X. Lei, B. Zhang, H. Zhang, Q. Zhang, *Compos. Sci. Technol.* **2018**, *167*, 79.
- [9] C. Pronoitis, M. Hakkarainen, K. Odelius, *Polym. Chem.* **2021**, *12*, 5668.
- [10] J. E. Mark, B. Erman, C. M. Roland, *The Science and Technology of Rubber*, 4th ed., Academic Press, Boston **2013**.
- [11] S. M. Clarke, F. Elias, E. M. Terentjev, *Eur. Phys. J. E: Soft Matter Biol. Phys.* **2000**, *2*, 335.
- [12] C. J. Kloxin, C. Bowman, *Chem. Soc. Rev.* **2013**, *2*, 7161.
- [13] L. Imbernon, E. K. Oikonomou, S. Norvez, L. Leibler, *Polym. Chem.* **2015**, *6*, 4271.

- [14] M. Zhang, F. Zhao, Y. Luo, *ACS Omega* **2019**, *4*, 1703.
- [15] G. Zhang, C. Tian, H. Feng, T. Tan, R. Wang, L. Zhang, *Macromol. Rapid Commun.* **2022**, *43*, 43.
- [16] M. Akiba, A. S. Hashim, *Prog. Polym. Sci.* **1997**, *22*, 475.
- [17] B. A. Dogadkin, A. A. Dontsov, *Vysokomol. Soedin.* **1961**, *3*, 1746.
- [18] B. A. Dogadkin, A. A. Dontsov, *Polym. Sci. USSR* **1965**, *7*, 1841.
- [19] H. Hinsken, S. Moss, J.-R. Pauquet, H. Zweifel, *Polym. Degrad. Stabil.* **1991**, *34*, 279.
- [20] H. Ahmad, D. Rodrigue, *Polym. Eng. Sci.* **2022**, *62*, 2376.
- [21] J. D. Andr s-Llopis, *J. Macromol. Sci. Part A Chem.* **1987**, *24*, 1263.
- [22] K. K. Jena, S. M. Alhassan, *J. Appl. Polym. Sci.* **2016**, *133*, 43060.
- [23] V. S. Wadi, K. Haliq, S. M. Alhassan, *Ind. Eng. Chem. Res.* **2020**, *59*, 13079.
- [24] B. A. Trofimov, T. A. Skotheim, A. G. Mal'kina, L. K. Sokolyanskaya, G. F. Myachina, S. A. Korzhova, E. S. Stoyanov, I. P. Kovalev, *Rus. Chem. Bull.* **2000**, *49*, 863.
- [25] B. A. Trofimov, *Sulfur Rep.* **2003**, *24*, 283.
- [26] L. Corbelli, in *Developments in Rubber Technology-2* (Eds: A. Whelan, K. S. Lee), Springer, Netherlands **1981**, p. 87.
- [27] A. E. Robinson, J. V. Marra, L. O. Amberg, *I&EC Product Res. Dev.* **1962**, *1*, 78.
- [28] C. G. Moore, B. R. Trego, *J. Appl. Polym. Sci.* **1957**, *1964*, 8.
- [29] E. Borsig, A. Fiedlerova, M. Lazar, *J. Macromol. Sci. Part A: Chem.* **1981**, *16*, 513.
- [30] C. Tzoganakis, J. Vlachopoulos, A. E. Hamielec, D. M. Shinozaki, *Polym. Eng. Sci.* **1989**, *29*, 390.
- [31] S. Coiai, E. Passaglia, M. Aglietto, F. Ciardelli, *Macromolecules* **2004**, *37*, 8414.
- [32] K. Naskar, J. Noordermeer, *Prog. Rubber Plast. Rec. Tech.* **2005**, *21*, 1.
- [33] G. Natta, G. Crespi, A. Valvassori, G. Sartori, *Rubber Chem. Technol.* **1963**, *36*, 1583.
- [34] M. Hernandez, A. M. Grande, W. Dierkes, J. Bijleveld, S. V. D. Zwaag, S. J. Garcaa, *ACS Sustain. Chem. Eng.* **2016**, *4*, 5776.
- [35] L. Gonzalez, A. Rodriguez, J. L. Valentın, A. Marcos-Fernandez, P. Posadas, *Kautschuk Gummi Kunststoffe* **2005**, *58*, 638.
- [36] W. Zhou, S. Zhu, *Ind. Eng. Chem. Res.* **1997**, *36*, 1130.
- [37] P. F. Lyons, T. C. Lee, A. V. Tobolsky, *J. Macromol. Sci. Part A: Chem.* **1968**, *2*, 1149.
- [38] F. A. Cotton, G. Wilkinson, C. Murillo, M. Bochmann, *The Group 16 Elements: S, Se, Te, Po*, 6th ed., John Wiley and Sons, Inc, New York **1999**, p. 496.
- [39] W. J. Chung, J. J. Griebel, E. T. Kim, H. Yoon, A. G. Simmonds, H. J. Ji, P. T. Dirlam, R. S. Glass, J. J. Wie, N. A. Nguyen, B. W. Guralnick, J. Park, A. Somogyi, P. Theato, M. E. Mackay, Y. E. Sung, K. Char, J. Pyun, *Nat. Chem.* **2013**, *5*, 518.
- [40] Y. Ikeda, *Understanding Network Control by Vulcanization for Sulfur Cross-Linked Natural Rubber (NR)*, Elsevier, Waltham, MA **2014**, p. 119.
- [41] M. A. D. Baez, P. J. Hendra, M. Judkins, *Spectrochim. Acta Part A* **1995**, *51*, 2117.
- [42] R. A. Nyquist, *Interpreting Infrared, Raman and Nuclear Magnetic Resonance Spectra*, Vol. 2, Elsevier, San Diego, CA **2001**, p. 65.
- [43] D. M. Byler, H. Susi, H. M. Farrell, *Biopolymers* **1983**, *22*, 2507.
- [44] J. Fan, G. Li, *RSC Adv.* **2017**, *7*, 1127.
- [45] R. G. W. Norrish, M. H. Searby, *Proc. Roy. Soc. London A: Math. Phys. Sci.* **1956**, *237*, 464.
- [46] G. Kar, M. O. Saed, E. M. Terentjev, *J. Mater. Chem. A* **2020**, *8*, 24137.
- [47] M. O. Saed, X. Lin, E. M. Terentjev, *ACS Appl. Mater. Interfaces* **2021**, *13*, 42044.
- [48] Y. Yang, E. M. Terentjev, Y. Wei, Y. Ji, *Nat. Commun.* **2018**, *9*, 1906.
- [49] F. Meng, M. O. Saed, E. M. Terentjev, *Macromolecules* **2019**, *52*, 7423.
- [50] C. Ruiz-Orta, J. P. Fernandez-Blazquez, A. M. Anderson-Wile, G. W. Coates, R. G. Alamo, *Macromolecules* **2011**, *44*, 3436.
- [51] I. Amer, Ph.D. Thesis, Stellenbosch University, **2011**.
- [52] M. Ratzsch, M. Arnold, E. Borsig, H. Bucka, N. Reichelt, *Prog. Polym. Sci.* **2002**, *27*, 1195.
- [53] Q. Shi, C. Jin, Z. Chen, L. An, T. Wang, *Adv. Funct. Mater.* **2023**, *33*, 2300288.
- [54] F. Meng, M. O. Saed, E. Terentjev, *Nat. Commun.* **2022**, *13*, 5753.
- [55] E. Bilgili, H. A. Adam Dybek, B. Bernstein, *J. Elast. Plast.* **2003**, *35*, 235.
- [56] H. P. Xiang, H. J. Qian, Z. Y. Lu, M. Z. Rong, M. Q. Zhang, *Green Chem.* **2015**, *17*, 4315.
- [57] E. Chabert, J. Vial, J.-P. Cauchois, M. Mihaluta, F. Tournilhac, *Soft Matter* **2016**, *12*, 4838.
- [58] C. W. Yeung, J. Y. Teo, X. J. Loh, J. Y. Lim, *ACS Mater. Lett.* **2021**, *3*, 1660.
- [59] G. Sagalayev, A. Dontsov, T. Suleimenov, *Polym. Sci. U.S.S.R.* **1973**, *15*, 2552.
- [60] V. S. Wadi, K. K. Jena, K. Haliq, S. M. Alhassan, *ACS Appl. Polym. Mater.* **2020**, *2*, 198.
- [61] C. N. R. Rao, R. Venkataraghavan, T. R. Kasturi, *Can. J. Chem.* **1964**, *42*, 36.

SUPPORTING INFORMATION

Additional supporting information can be found online in the Supporting Information section at the end of this article.

How to cite this article: C. Houghton-Flory, M. O. Saed, E. M. Terentjev, *J. Polym. Sci.* **2024**, *1*, <https://doi.org/10.1002/pol.20230869>